Fabrication and characterization of photodetector based on tellurium oxide thin film

G. AKRAM*, S. KADHIM , H. ABDULLAH*
Laser and Optoelectronics Engineering Department, University of Technology-Iraq, Baghdad, Iraq

For the fabrication of the inorganic TeO_2/Si heterojunction, thermal vapor deposition was employed. By varying the annealing temperature to 100°C, 125°C, 150°C, and 175°C, the optoelectronic properties of the photodetector were studied. The heterojunctions annealed at 175 °C exhibited outstanding performance, including a notable quantum efficiency value of 74.747% with an applied reverse bias of (−2 V), and an outstanding detectivity of ($2.502x10^{11}$cm.Hz $^{1/2}$.W^{-1}). TeO_2 nanoscale thin films manufactured by a vacuum deposition approach demonstrated high durability. The (I–V) characteristics of the TeO_2/Si heterojunction were verified in the dark and at room temperature.

(Received December 9, 2022; accepted June 9, 2023)

Keywords: Photodetector, TeO_2, Nanoparticles, Electrical properties

1. Introduction

The development of photodetectors is currently heavily focused on how to scale them down to the nanoscale for technological applications in order to create a highly integrated and high-performance photodetection system [1]. A novel design of nanostructures with very effective incoming light absorption and hot electron production is selected in order to boost the quantum efficiency of the photodetection. Utilizing fresh substances like low-dimensional materials would also increase the spectrum range of light absorption and hot-electron creation, effectively turning light into current signals [2]. Semiconductor photodetectors have been widely utilized with the expansion of photoelectronic applications. The development of new materials and new structures like heterojunctions and quantum wells has sparked an increase in research into semiconductor materials [3]. Due to its small band gap of 1.12 eV, silicon responds to broad-band light with a wavelength range of 400nm to 1100nm. Many researchers have focused on these materials since silicon's microelectronic technology has established a strong foundation for silicon-based heterojunction materials [4].

In order to fulfill future needs in a number of industries, next generation photodetectors will need major increases in sensitivity, selectivity, and stability. Despite the fact that certain research teams have successfully used metal oxide nanostructures to detect light, the selectivity and stability are still rather low. Although significant efforts have been made to create high-quality metal oxide nanostructures, there are still many difficulties in doing so. These difficulties include, but are not limited to, the inability to reliably control length, diameter, orientation, crystallization, density and hierarchical assembly [5].

Tellurium dioxide (TeO2) was chosen for the manufacture of the photodetector in this study. TeO2, an important acousto-optical material, has elastic behavior, a high refractive index, and excellent optical quality. We used the thermal evaporation method to make homogeneous deposition and high-quality TeO2 thin films. Then, annealing was carried out at various temperatures (100°C, 125°C, 150°C, and 175°C) that caused enhancements in the electrical properties of the thin films. We investigated high efficiency and good responsiveness over a wide range in the visible region.

2. Material and method

The thermal evaporation technique shown fig.1, was employed to produce thin films of TeO_2 on N-type silicon wafer substrates with a thickness of (525 ±25) μm which is used to study the photovoltaic and electrical properties of heterojunction. Fig. 2 illustrates the molybdenum boat that was used to vaporize the TeO_2 powder. The best distance between the substrates and the boat is 15 cm to achieve homogeneous deposition. For this purpose, a high degree of purity 99.99 percent (approximately one gram) of TeO_2 powder was loaded. Keeping the vacuum chamber at a vacuum pressure of 10^{-5} (mbar) during film deposition after the end of the evaporation process, leave the sample in the chamber to cool and then extract it for the annealing process.

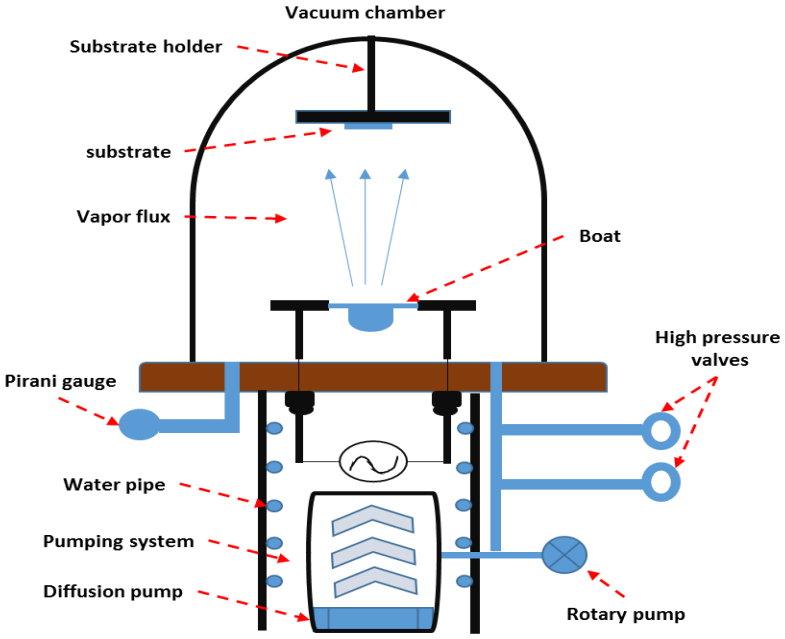

Fig. 1. Thermal vapor deposition system (color online)

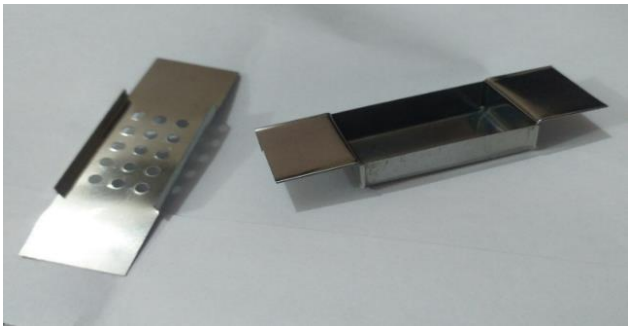

Fig. 2 Molybdenum boat (color online)

Finally, TeO_2 thin films were annealed in an electric furnace that shown in Fig. 3 at temperatures of 100ºC, 125ºC, 150ºC, and 175ºC degrees Celsius. As shown in Fig. 4 high purity aluminum powder 99.99% percent was used to achieve the ohmic contact necessary to measure the electrical properties of the thin films. To obtain electrodes, three grams of aluminum powder are placed in a tungsten boat and, by the process of thermal evaporation, keeping the vacuum in the chamber on the order of 10^{-5} (mbar), the electrodes are deposited on the previously prepared mask. The electrical properties of TeO_2 and TeO_2/Si heterojunction films were studied.

Fig. 3. Electric furnace (color online)

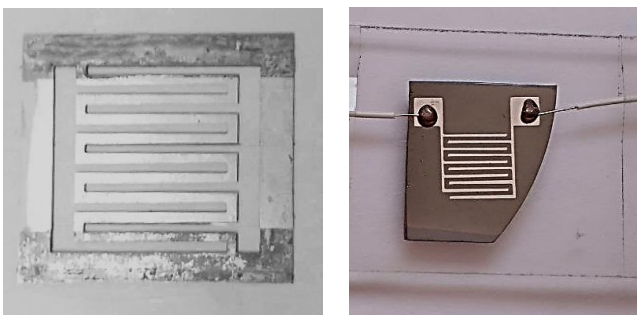

Fig. 4. Device fabrication and metallization (color online)

3. Results and discussion

3.1. Hall effect measurements

By examining the Hall Effect (R_H), it is possible to determine the type of charge carriers as well as their mobility (μ_H) and carrier concentration (C.C). The results showed that all TeO_2 thin films prepared at annealing temperatures of 100°C, 125°C, 150°C, and 175°C are p-type semiconductors [6]. The concentration of charge carriers (C.C) tends to increase with increasing annealing temperature. The corresponding rise in average grain size is the reason for this [7]. Defects decrease with increasing grain size, which leads to a decrease in resistance (R). In addition, since there is a relationship between carrier concentration (C.C) and conductivity (σ), we observe an increase in Hall mobility (μ_H) with increasing annealing temperature. In other words, the mobility is size-dependent and found to be (117.2 cm^2 V^{-1} s^{-1}) at 175 C. The results are comparable with those in other studies [8]. Table 1 depicted Hall Effect measurements.

Table 1. Hall effect measurements

T °C	C.C (cm^{-3})	μ_H (cm^2/v. s)	R(Ω)	σ (Ω. cm)$^{-1}$	R_H(m^2/ C)
100	8.61E +17	9.378E +01	5.18E +01	1.292E +01	7.259E +00
125	9.42E +17	1.036E +02	4.71E +01	1.562E +01	6.634E +00
150	1.05E +18	1.059E +02	3.27E +01	1.782E +01	5.942E +00
175	1.12E +18	1.172E +02	3.98E +01	2.099E +01	5.58E+ 00

3.2. Electrical properties of (TeO_2 /Si) heterojunction

3.2.1. I-V characteristics (TeO_2 /Si) heterojunction

The (I-V) characteristics of TeO_2/Si prepared at various annealing temperatures are shown in Fig.5. All photodetectors clearly have two regions for the forward current. The current drawn by each photodetector in the first low voltage region is very low. Recombination current only happens at low voltage and is known for that as well. It is created when every electron that has been excited from the valance band to the conduction band recombines with a hole there to restore balance. Due to the bias voltage potential exceeding the potential barriers in the second region of high voltage, the forward current increases exponentially. The electron has sufficient energy from this bias voltage to cross the barrier height and flow. The diffusion current is referred to as that. While in reverse bias, the dominance of edge leakage current, which is provided by the sharp edge at the contact's boundary and is also brought on by the generation of excess carriers in the depletion region, was found to cause the current to increase slowly with voltage [9].

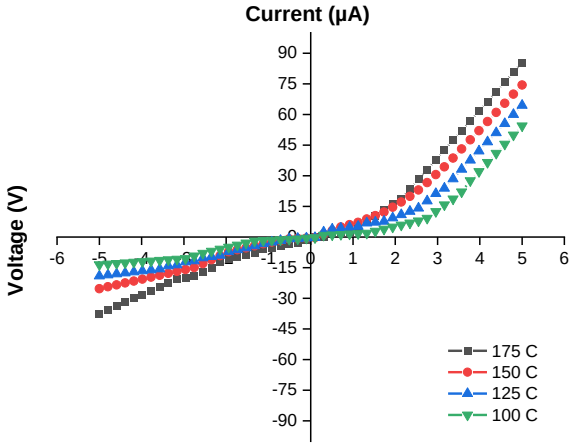

Fig. 5. I-V characteristics of (TeO_2/Si) heterojunction at various annealing temperatures (color online)

3.2.2. Capacitance–voltage characteristics of (TeO_2 /Si) heterojunction

In Fig. 6, junction capacitance for (TeO_2 /Si) heterojunction synthesized at various annealing temperatures is shown to vary with reverse bias voltage in the range of (0-2) V. It has been found that as the bias voltage rises, the capacitance falls off exponentially. This behavior is explained by the fact that the depletion region widens with bias voltage, causing the capacitance at the junction sides to decrease, so that the value of the built in potential is increased [10].

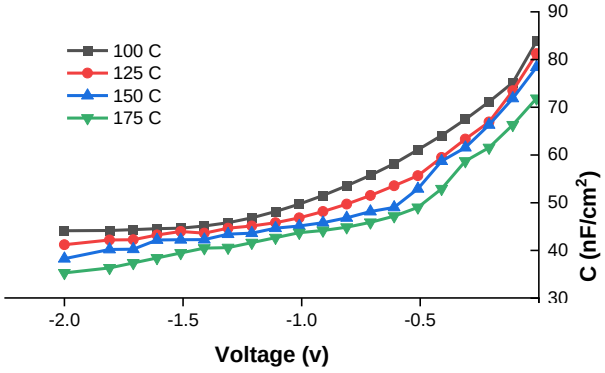

Fig. 6. C-V characteristics of (TeO_2/Si) heterojunction as a function of reverse bias voltage at various annealing temperatures (color online)

Fig. 7 depicts the relationship between the (TeO_2/Si) heterojunction's square of the inverse capacitance is plotted against the applied reverse bias voltage for samples made at various annealing temperatures in the dark and at room temperature. The built-in potential (V_{bi}) was determined by extrapolating the linear part of the $1/C^2$ to the zero point as recorded in Table 2. As a result, an abrupt junction is formed between the TeO_2 thin film and the Si substrate. These results demonstrate that the capacitance at zero bias

voltage (C_0) decreases during annealing, and this is attributed to increases in the depletion layer [11].

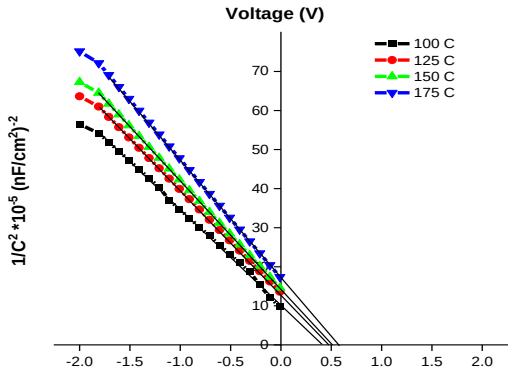

Fig. 7. The variation of $1/C^2$ of (TeO_2/Si) heterojunction as a function of reverse bias voltage at various annealing temperatures (color online)

Table 2. The built-in potential V_{bi} at different annealing temperatures

Annealing Temperature (°C)	Built in potential V_{bi} (V)
175	0.565
150	0.503
125	0.468
100	0.417

3.3. TeO2 /Si detectors measurements

3.3.1. Spectral responsivity (R_λ)

Spectral responsivity (R_λ) is the most crucial factor in determining the range of hetero-junction operation and whether it is suitable for detectors. The spectral responsivity of (TeO_2/Si) heterojunctions prepared at various annealing temperatures and examined in the wavelength range of (350-1000) nm is shown in Fig.8. It is evident that the responsivity of the TeO_2/Si device is relatively low when the wavelength is 500 nm or less. The maximum photo-responsivity peaked at about (505, 595, 625, and 660) nm for temperatures (100, 125, 150, and 175) °C, respectively. The peaks of (R_λ) are shifted to longer wavelengths as a result of the decrease in resistance and the increased photocurrent, and the spectral responsiveness value increases with increasing annealing temperature[12]. The photocurrent measurement reflects the relationship between the response spectrum and the energy band structure of TeO_2. The electron-hole pairs excited by the incident beam with energy greater than the band gap are thought to be the cause of the increased spectral responsiveness [13]. A significant increase in conductance can only be brought about by a photon with sufficient energy. A photon with less energy cannot excite electrons in the conduction band to move them from the valence band, and as a result, it has little effect on the photocurrent [14]. The transient increase in response on the long wavelength side may be brought on by carriers moving from intrinsic defects in the band gap to the conduction band [15]. The increased absorption of high energy photons at the semiconductor surface region is the cause of the reduced responsivity on the shorter wavelength side. Since the lifetime of the electron-hole pairs created close to the surface region is typically shorter than that of those in the bulk, they have a smaller impact on photo-conductance [16].

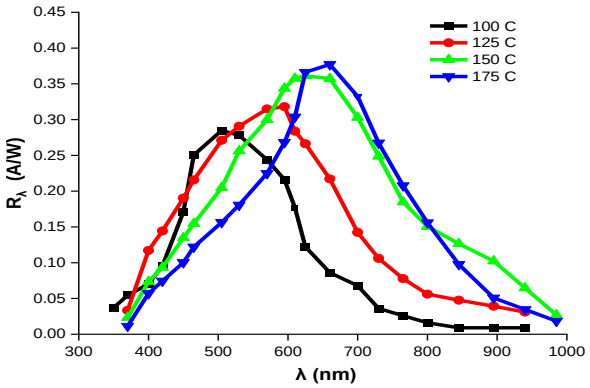

Fig. 8. The spectral responsivity as a function of wavelength of (TeO_2/Si) heterojunctions at various annealing temperatures (color online)

3.3.2. Quantum efficiency (η)

Quantum efficiency is a quantity that defines the ratio between the number of induced electrons in the heterojunction and the number of incident photons in the practical area of the heterojunction [17]. The following equation relates the quantum efficiency to the spectral responsivity [18]:

$$\eta = R(\lambda)\frac{h\,c}{q\,\lambda} \quad (1)$$

where is (q) is the charge of electron, and (hc) is the energy of photon. TeO_2/Si heterojunction quantum efficiency at various annealing temperatures is depicted in Fig.9 as a function of wavelength. The maximum quantum efficiency (74.747%) at about 625nm for temperature 175C.

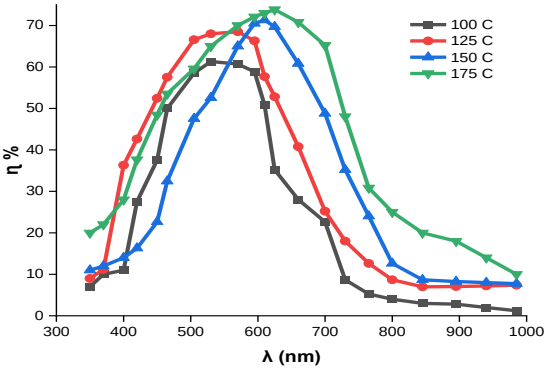

Fig. 9. Quantum efficiency as a function of wavelength for TeO_2/Si heterojunctions at various annealing temperatures (color online)

3.3.3. Specific detectivity (D)*

Specific detectivity values were calculated according to the equation [19]:

$$D^* = R_\lambda \left(\frac{S}{2qI_d}\right)^{0.5} \quad (2)$$

Where (S) is the area of the sample, and (I_d) is the dark current.

The change in the detectivity with the wavelength for TeO_2/Si heterojunctions at different annealing temperatures is shown in Fig.10 and Table 3. It is evident that the specific detectivity increases with increasing annealing temperature, where the highest value of the detectivity (2.502×10^{11} cm.Hz $^{1/2}$.W^{-1}) at about 625nm for a temperature of 175 C. The interpretation of that is due to a decrease in the defect that conducts to a decrease in the recombination centers, which influences the value of specific detectivity and decreases the noise current due to the decrease in dark current.

Table 3. The values of R_λ, η % and D for TeO_2/Si detectors at different annealing temperatures*

T °C	(R_λ) (Amp/W)	(η) (%)	(D*) (cm.Hz $^{1/2}$.W^{-1})
100	0.244	57.086	2.085E+11
125	0.318	69.178	2.284E+11
150	0.361	73.338	2.322E+11
175	0.377	74.747	2.502E+11

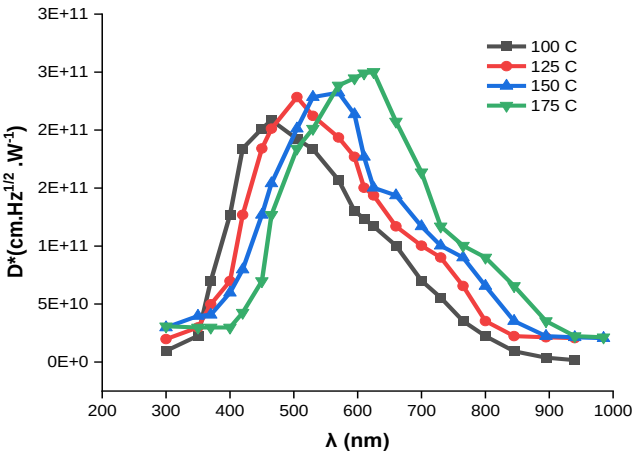

Fig. 10. The change in the detectivity with the wavelength for TeO_2/Si heterojunctions at different annealing temperatures (color online)

4. Conclusion

Nanoscale TeO2 particles have been successfully prepared using the thermal evaporation deposition process. The tellurium oxide films underwent thermal annealing, which improved the material's electrical properties and increased the photodetector's efficiency to 74.747% at 175 °C. In order to increase the concentration of charge carriers, we observe that the electrical conductivity of the TeO_2 thin films increases with an increase in the annealing temperature. This is a characteristic of semiconductors. The visible spectrum of wavelengths, where the incident photon's energy was absorbed most efficiently, showed the device's highest response.

References

[1] E. T. Salem, M. A. Fakhry, H. Hassen, Int. J. Nanoelectron. Mater. **6**(2), 121 (2013).
[2] Z. M. Wei, J. B. Xia, Acta Phys. Sin. **68**(16), 393 (2019).
[3] L. Yang, S. Wang, Q. Zeng, Z. Zhang, L. M. Peng, Small **9**(8), 1225 (2013).
[4] Z. Xu, S. Lin, X. Li, S. Zhang, Z. Wu, W. Xu, Y. Lu, S. Xu, Nano Energy **23**, 89 (2016).
[5] T. Zhai, X. Fang, M. Liao, X. Xu, H. Zeng, B. Yoshio, D. Goldberg, Sensors **9**(8), 6504 (2009).
[6] K. Doi, T. Sasaki, K. Hijikata, Bulletin of the Chemical Society of Japan **48**(1). 144 (1975).
[7] M. Miyake, K. Murase, T. Hirato, Y. Awakura, J. Electroanal. Chem. **562**(2), 247 (2004).
[8] G. Upender, V. Chandra Mouli, J. Mol. Struct. **1006**(1-3), 159 (2011).
[9] M. Soylu, H. S. Kader, J. Electron. Mater. **45**(11), 5756 (2016).
[10] A. M. Mousa, S. M. Hassen, S. Mohmoed, Int. Lett. Chem. Phys. Astron. **34**(1), 1 (2014).
[11] H. M. Zeyada, M. M. El-Nahass, M. A. Ali, EPJ Appl. Phys. **56**(1), 1 (2011).
[12] H. Hassan, K. I. Hajim, One Dimensional Tight Binding Computations for CNT Type, Diameters and Chirality at (1550, 1300) nm Communication Window Wavelength, 1 (2014).
[13] Z. Fan, P.-C Chang, J. G. Liu, E. C. Walter, R. M. Penner, C.-H. Liu, H. P. Lee, Appl. Phys. Lett. **85**(25), 6128 (2004).
[14] D. P. Amalnerkar, Mater. Chem. Phys. **60**(1), 1 (1999).
[15] J. S. Jie, W. J. Zhang, Y. Jiang, X. M. Meng, Y. Q. Li, S. T. Lee, Nano Lett. **6**(9),1887 (2006).
[16] E. Stamate, Nanomaterials **10**(1), 1 (2020).
[17] E. F. Zalewski, C. R. Duda, Appl. Opt. **22**(18), 2867 (1983).
[18] S. E. Shaheen, C. J. Brabec, N. S. Sariciftci, F. Padinger, T. Fromherz, J. C. Hummelen, Appl. Phys. Lett. **78**(6), 841 (2001).
[19] Z. Song, Y. Liu, Q. Wang, S. Yuan, Y. Yang, X. Sun, Y. Xin, M. Liu, Z. Xia, J. Mater. Sci. **53**(10), 7562 (2018).

* Corresponding authors: ghadeerakram98@gmail.com; Hiba.H.Abdullah@uotechnology.edu.iq